

Dynamic patterns of histone H3 lysine 4 methyltransferases and demethylases during mouse preimplantation development

Gen-Bao Shao · Jun-Chao Chen · Liu-Ping Zhang ·
Pan Huang · Hong-Yan Lu · Jie Jin · Ai-Hua Gong ·
Jian-Rong Sang

Received: 1 December 2013 / Accepted: 16 February 2014 / Published online: 12 March 2014 / Editor: T. Okamoto
© The Society for In Vitro Biology 2014

Abstract Extensive and dynamic chromatin remodeling occurs after fertilization, including DNA methylation and histone modifications. These changes underlie the transition from gametic to embryonic chromatin and are thought to facilitate early embryonic development. Histone H3 lysine 4 methylation (H3K4me) is an important epigenetic mechanism that associates with gene-specific activation and functions in development. However, dynamic regulation of H3K4me during early embryonic development remains unclear. Herein, the authors examined the dynamic changes of H3K4me and its key regulators (*Ash1l*, *Ash2l*, *Kmt2a*, *Kmt2b*, *Kmt2c*, *Setd1a*, *Setd7*, *Kdm1a*, *Kdm1b*, *Kdm5a*, *Kdm5b*, *Kdm5c*, and *Kdm5d*) in mouse oocytes and preimplantation embryos. An increase in levels of H3K4me₂ and me₃ was observed at the one- to two-cell stages ($P < 0.05$), corresponding to the period of embryonic genome activation (EGA). Subsequently, the H3K4me₂ level dramatically decreased at the four-cell stage and remained at low level until the blastocyst stage ($P < 0.05$), whereas the H3K4me₃ level transiently decreased in the four-cell embryos but steadily increased to the peak in the blastocysts ($P < 0.05$). The high level of H3K4me₂ during the EGA

was coinciding with a peak expression of its methyltransferase, ASH2L, which may stabilize this methylation level during this period. Correspondingly, a concomitant decrease in levels of its demethylases, KDM5B and KDM1A, was observed. H3K4me₃ was correlated to the expression of its methyltransferase (KMT2B) and demethylase (KDM5A). Thus, these enzymes may function for the EGA and the first lineage segregation in preimplantation mouse embryos.

Keywords Demethylase · Histone H3 methylation · Methyltransferase · Preimplantation embryo

Introduction

Epigenetic modifications, such as DNA methylation, histone methylation, and acetylation, regulate the patterns of gene expression through the changes of chromatin structure and DNA accessibility (Beisel and Paro 2011). The methylation of lysine 4 of histone H3 (H3K4me) is one of these modifications, which is involved in gene activation (Eissenberg and Shilatifard 2010). Specifically, H3K4 di- and trimethylation (H3K4me₂ and me₃) residues mark the transcription start sites of actively transcribed genes (Bernstein et al. 2006; Barski et al. 2007; Mikkelsen et al. 2007), while high level of H3K4 monomethylation (H3K4me₁) is associated with enhancer sequences (Heintzman et al. 2007). H3K4me_{2/3} has also been shown to regulate the expression of pluripotency genes (Pan et al. 2007; Wang et al. 2009a, b) and *Hox* genes (VerMilyea et al. 2009) in mouse preimplantation embryos and embryonic stem cells.

Epigenetic regulation of gene expression is mediated primarily by SET-domain- and JmjC-domain-containing proteins. The SET/mixed lineage leukemia (MLL) family of SET proteins is primarily responsible for the generation of H3K4me_{1/2/3} to induce gene activation, and it has seven major members as follows: lysine (K)-specific

G.-B. Shao (✉) · J.-C. Chen · L.-P. Zhang · J. Jin · A.-H. Gong
Department of Biology, School of Medical Science and Laboratory
Medicine, Jiangsu University, 301 XueFu, Zhenjiang 212013, China
e-mail: genbaoshao@163.com

P. Huang
Department of Pathology, School of Medical Science and Laboratory
Medicine, Jiangsu University, Zhenjiang 212013, China

H.-Y. Lu
Department of Pediatrics, The Affiliated Hospital of Jiangsu
University, Zhenjiang 212001, China

J.-R. Sang
Department of Physiology, School of Medical Science and
Laboratory Medicine, Jiangsu University, Zhenjiang 212013, China

methyltransferase 2A (KMT2A)/MLL1, KMT2B/MLL2, KMT2C/MLL3, ASH1L, ASH2L, SETD1A, and SETD7 (Dou et al. 2006; Black et al. 2012). In contrast, the lysine (K)-specific demethylase 5 (KDM5) family of JmjC proteins (KDM5A/RBP2, KDM5B/PLU1, KDM5C/SMCX, and KDM5D/SMCY) has recently been identified as demethylases of H3K4me_{2/3} causing gene repression (Klose et al. 2006). In addition, KDM1A/LSD1 and KDM1B/LSD2 demethylate H3K4me_{1/2} and result in gene repression (Shi et al. 2004; Fang et al. 2010).

The families of MLL methyltransferases and KDM5 demethylases are essential for normal development in mammals. Loss of either *Kmt2a* or *Kmt2b* in oocytes results in anovulation and oocyte death (Terranova et al. 2006; Andreu-Vieyra et al. 2010). Knockout of *Ash2l* or *Kdm5b* causes early embryonic lethality (Stoller et al. 2010; Albert et al. 2013). In the absence of *Kdm1b*, germ cells do not undergo de novo DNA methylation during oogenesis (Ciccone et al. 2009), while *Kdm1a* deficiency causes embryonic lethality due to a progressive loss of genomic DNA methylation and therefore lack of cell differentiation (Wang et al. 2009a, b). Inhibition of KDM1A also results in early embryo arrest in our previous studies (Shao et al. 2008a). Recently, *Kdm1a* mutants display germline sterility and defects in ovary development (Di Stefano et al. 2007; Katz et al. 2009; Eliazar et al. 2011). More recently, antagonistic functions of *Kdm5a* and *Ash2l* regulate lifespan and control a set of genes involved in lifespan determination (Greer et al. 2010). These studies suggest that the dynamic regulation of the H3K4me state continues throughout early development. However, the embryonic expression of these epigenetic regulators has not been well investigated, especially in early developmental stages.

Here, we investigated the levels of H3K4me in preimplantation mouse embryos, and performed quantitative real-time polymerase chain reaction (PCR) analyses of the messenger RNA (mRNA) expression of *Ash1l*, *Ash2l*, *Kmt2a*, *Kmt2b*, *Kmt2c*, *Setd1a*, *Setd7*, *Kdm1a*, *Kdm1b*, *Kdm5a*, *Kdm5b*, *Kdm5c*, *Kdm5d*, *H2afz*, and *Gapdh* (Table 1). Furthermore, immunofluorescence was performed to analyze the protein expression of these regulators to find out their association with the levels of H3K4me.

Materials and Methods

Animals. Kunming (KM) white female mice (3–4 wk old) and imprinting control region (ICR) male mice (12–16 wk old) were obtained from the Experimental Animal Breeding Center of Jiangsu University. All animals were maintained under controlled temperature (25±2°C) and lighting (light from 0700 to 1900 h) for at least 1 wk prior to use. Animal care and experimental procedures were conducted in accordance with the Animal Research Committee Guidelines of Jiangsu University.

Reagents and media. All reagents and media used in this study were from Sigma-Aldrich Inc. (St. Louis, MO) unless noted otherwise. M2 (M7167; Sigma-Aldrich) and KSOM (MR-020P-5F; Millipore, Billerica, MA) media were prepared for the handling and culture of mouse oocytes and embryos, respectively.

Oocyte collection. To retrieve fully grown oocytes arrested at prophase I of meiosis, KM white mice were treated with 10 IU of pregnant mare serum gonadotrophin (PMSG; Ningbo Second Hormone Factory, Zhejiang, China). The ovaries were removed from the mice 48 h after PMSG treatment and transferred to M2 medium. The ovarian follicles were punctured with a 30-gauge needle to release the oocytes in the cumulus oophorus. The cumulus cells surrounding the oocytes were removed by gentle pipetting through a narrow glass pipette in the M2 medium. Oocytes showing germinal vesicles (GVs) were collected.

Mature oocytes were retrieved by treatment with 10 IU of PMSG followed by 10 IU of human chorionic gonadotropin (hCG; Ningbo Second Hormone Factory) 48 h later. Cumulus oocyte complexes (COCs) were collected from the ampulla of oviducts 15 h after hCG injection, placed in M2 medium, and treated with 0.1% hyaluronidase until the cumulus cells dispersion.

In vivo-derived embryo collection. Female KM white mice were treated with 10 IU of PMSG followed by 10 IU of hCG 48 h later. Immediately after the hCG injection, the mice were mated overnight with ICR male mice. Embryos were harvested from pregnant mice at 18, 42, 50, 62, 76, and 90 h post-hCG injection to obtain the one-cell, two-cell, four-cell, eight-cell, morulae, and blastocysts stages, respectively. One-cell, two-cell, four-cell, eight-cell, and morulae stages were flushed from oviducts with prewarmed M2 medium and cultured in KSOM medium. Blastocysts were retrieved by flushing uterine horns. The recovered embryos were placed in RNA extraction buffer and stored at –80°C.

mRNA extraction and complementary DNA (cDNA) synthesis. Polyadenylated mRNA was extracted from pools (30) of embryos of the respective developmental stage using PicoPure RNA Isolation Kit (Arcturus, Molecular Devices, Mountain View, CA). Polyadenylated mRNA was extracted from pools of embryos collected on a single day. Each mRNA extraction was replicated three times for each experiment. Oocytes and embryos were washed three times in PVA-PBS and then lysed in 20 µl of extraction buffer at 42°C for 30 min and stored at –80°C until mRNA isolation. The mRNAs were reverse transcribed following the manufacturer's instructions using PrimeScript RT Reagent Kit (Takara, Shiga, Japan).

Table 1. Information on genes studied

Gene	Relevant information	Gene ontology
<i>Ash1l</i> and <i>Ash2l</i>	Absent, small, or homeotic 1/2-like (<i>Drosophila</i>). <i>Ash1l</i> and <i>Ash2l</i> are highly similar. <i>Ash1l</i> associates with the transcribed region of active genes and is essential for H3K4 methylation (Gregory et al. 2007). <i>Ash2l</i> is a core subunit of MLL methyltransferase complex and is a key regulator of open chromatin (Wan et al. 2013).	Methyltransferase activity Chromatin modification Transcription activation
<i>Kmt2a</i> , <i>Kmt2b</i> and <i>Kmt2c</i>	Lysine (K)-specific methyltransferase 2a, 2b and 2c. <i>Kmt2a</i> and <i>Kmt2b</i> are highly homologous. They form similar KMT complexes and both are required for accurate regulation of gene expression and oocyte development (Milne et al. 2002; Andreu-Vieyra et al. 2010). <i>Kmt2c</i> is a component of the ASC-2/NCOA6 (ASCOM) complex and is involved in transcriptional coactivation (Lee et al. 2008). <i>Kmt2a-c</i> share a common core, formed by <i>Wdr5</i> , <i>RbBP5</i> , <i>Dpy-30</i> , and <i>Ash2l</i> , and possess methyltransferase activity toward H3K4.	Methyltransferase activity Chromatin modification Regulation of transcription
<i>Setd1a</i> and <i>Setd7</i>	SET (Su(var)3-9, enhancer of zeste, trithorax) domain containing 1a and 7. Both contain SET domains which catalyze the methylation of histone and non-histone proteins (Dillon et al. 2005). SETD1A interacts with RNA polymerase II (RNAP II) C-terminal domain and mediates histone H3K4 methylation at a subset of transcriptionally active genes (Lee and Skalnik 2008). SETD7 monomethylates histone H3K4 and predominately associates with active chromatin. Moreover, SETD7 also methylates DNMT1 leading to proteasome mediated protein degradation, and antagonist KDM1A, prevents this degradation by removing the methyl mark (Pradhan et al. 2009).	Methyltransferase activity Chromatin modification Transcription activation
<i>Kdm1a</i> and <i>Kdm1b</i>	Lysine (K)-specific demethylase 1a and 1b. KDM1A demethylates H3K4me1/2 via FAD-dependent oxidative reaction, and has been linked in a number of corepressor complexes (Shi et al. 2004). <i>Kdm1b</i> , a gene related to <i>Kdm1a</i> , functions as a H3K4 demethylase and is required for de novo DNA methylation of some imprinted genes (Ciccone et al. 2009).	Demethylase activity Chromatin modification Regulation of transcription
<i>Kdm5a</i> , <i>Kdm5b</i> , <i>Kdm5c</i> and <i>Kdm5d</i>	Lysine (K)-specific demethylase 5a, 5b, 5c, and 5d. <i>Kdm5a</i> and <i>Kdm5b</i> enhance nuclear hormone receptor-mediated transcription (Chan and Hong 2001; Xiang et al. 2007) whereas <i>Kdm5b</i> also has transcriptional repression activity (Yamane et al. 2007). <i>Kdm5c</i> and <i>Kdm5d</i> have been identified as E2-dependent regulators of oncogene expression and implicated in X-linked mental retardation (Jensen et al. 2005; Smith et al. 2010). These demethylases contain a JmjC domain which is known for histone demethylation (Klose et al. 2006).	Demethylase activity Chromatin modification Regulation of transcription Transcription activity
<i>H2afz</i> and <i>Gapdh</i>	H2A histone family, member Z (<i>H2afz</i>); Glyceraldehydes-3-phosphate dehydrogenase (<i>Gapdh</i>). <i>H2afz</i> and <i>Gapdh</i> genes are the most stable expression in the in vivo and in vitro derived preimplantation-stage mouse embryos (Mamo et al. 2007; Wang et al. 2010).	Housekeeping genes

Real-time PCR. The quantification of all gene transcripts was carried out in three replicate by quantitative real-time PCR on the Bio-Rad CFX96 system using SsoFast EvaGreen Supermix (Bio-Rad, Hercules, CA). The primer sequences for each gene are listed in Table 2. Primers for *Kdm5a*, *Kdm5b*, *Kdm5c*, *Kdm1a*, *Kdm1b*, *Ash1l*, and *Kmt2a* were designed using Primer Premier 5.0 based on available sequences from Database of GenBank (NCBI). Primers for *Kdm5d*, *Ash2l*, *Kmt2b*, *Kmt2c*, *Setd1a*, *Setd7*, *H2afz*, and *Gapdh* were referred to previous literatures (VerMilyea et al. 2009; Andreu-Vieyra et al. 2010; Wang et al. 2010; Albert et al. 2013). The reaction mixture of the total 20 μ l volume consisted of 10 μ l of 1 \times SsoFast EvaGreen Supermix, 1 μ l of each primer (0.5 μ M),

6 μ l of RNase/DNase-free water, and 2 μ l of cDNA template. The PCR was conducted in an initial step of 95°C for 30 s, 40 cycles of 95°C for 5 s, and 58–60°C for 5 s. The fluorescence values were determined after each elongation step. The dissociation curve was analyzed following the final cycle to determine the specificity of amplification. The melting protocol consisted of heating from 65°C to 95°C, holding at each temperature for 0.1 s while monitoring fluorescence. To identify specific amplification of a single PCR product, the product was confirmed by 2% agarose gel electrophoresis. Negative controls, comprised of the PCR reaction mix, without nucleic acid, were also run with each group of samples. The comparative cycle threshold method was used for quantification of expression levels. The abundance of

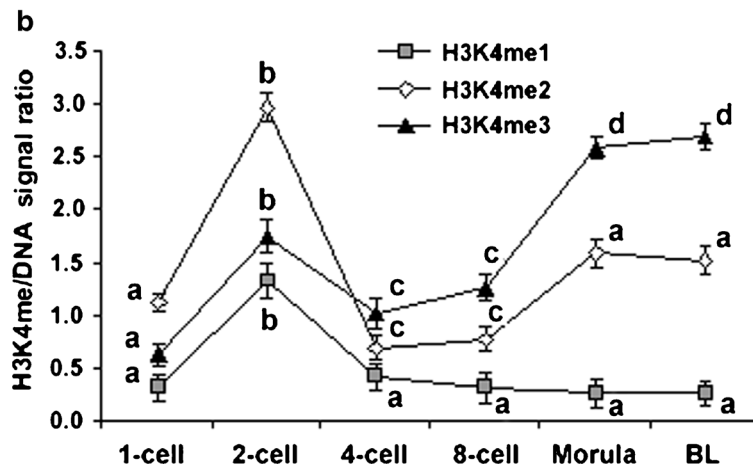
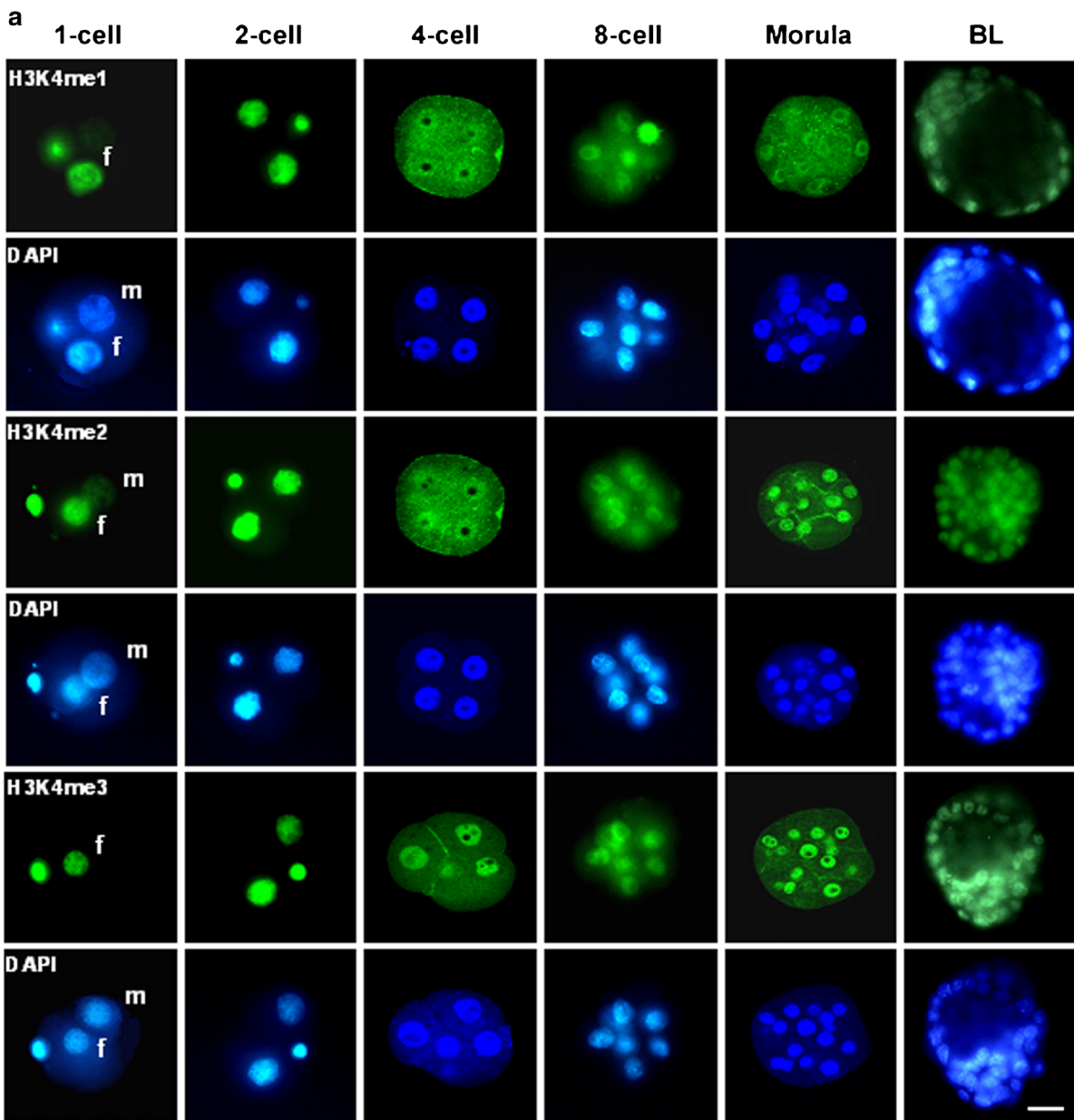
Table 2. Primers used for quantitative real-time PCR

Gene	Primer type	Primer sequence (5'-3')	Fragment size (bp)	NCBI accession number
<i>Kdm5a</i>	Sense	GGTGTATCCGCAGAAATGG	105	NM_145997.2
	Antisense	TAGGAAGGGAGGAGGTGGT		
<i>Kdm5b</i>	Sense	CAGGAGTTGCTGGATGTCA	134	NM_152895.2
	Antisense	AAAGAAAGGGAGCTGGAGT		
<i>Kdm5c</i>	Sense	GGCAGAAGCATCCACCAGC	179	NM_013668.3
	Antisense	GCCCTCCAAGTCATCCAAGCA		
<i>Kdm5d</i>	Sense	GAGTATGGAGATGCCGAAG	126	NM_011419.3
	Antisense	CCTGAAGGAGTCAGCCATC		
<i>Kdm1a</i>	Sense	GGTCTTATCAACTTCGGCATCT	176	NM_133872.2
	Antisense	GCAACTCGTCCACCTACTCG		
<i>Kdm1b</i>	Sense	CGAGGATCTGAGAGTGCTGGA	152	NM_172262.3
	Antisense	GATGTGTGCTGGTGCAGGA		
<i>Ash1l</i>	Sense	GCTACCTGTCTCTCTCC	173	NM_138679.5
	Antisense	AACCCAACTGCTGTGCTA		
<i>Ash2l</i>	Sense	GCAAGCACTATTCGTCTGGCT	104	BC012957.1
	Antisense	TTGTAGGTGTCCGGCAGTGA		
<i>Kmt2a</i>	Sense	AAGCCACCTCCAGTAAAGTAA	176	NM_001081049.1
	Antisense	ATCCCTAAGCCTCCCATC		
<i>Kmt2b</i>	Sense	TGTTGCATGAAAACGCC	118	AB182318.1
	Antisense	TGCAAGTGGCAGCAAAGGA		
<i>Kmt2c</i>	Sense	CCCCAATTGCCCAACTATCT	158	NM_001081383.1
	Antisense	TCGTAAGCGTTCTTCTCTCTCT		
<i>Setd1a</i>	Sense	GCGACTCACATATGAACGGCT	107	NM_178029.3
	Antisense	TGCGCTTTGGAGTGCTTAGG		
<i>Setd7</i>	Sense	TCTCCAAGGCACCTATGTGGA	118	NM_080793.5
	Antisense	CCAACACACTCCGTGTCGATT		
<i>H2afz</i>	Sense	CCAAGACAAAGCGGTTTCC	176	NM_016750.2
	Antisense	TCCTGCCAACTCAAGTACCTC		
<i>Gapdh</i>	Sense	TGGCAAAGTGGAGATTGTTGCC	156	GU214026.1
	Antisense	AAGATGGTGTATGGGCTTCCCG		

each single gene was determined relative to the averages of two housekeeping genes (*H2afz* and *Gapdh*). Fluorescence was acquired in each cycle to determine the threshold cycle (C_T), the cycle during the log-linear phase of the reaction at which fluorescence was increased above background for each sample. The sample ΔC_T value was calculated by the difference between the average C_T value and the sample C_T value. The GV stage was used as the calibrator and used subsequently to obtain $\Delta\Delta C_T$ values. Fold differences of the gene expression were determined by using the formula $2^{-\Delta\Delta C_T}$.

Immunofluorescence analysis. Embryos were fixed with 3.7% paraformaldehyde in PBS for 30 min at room temperature. After three 30-min washings in PBS containing 0.1% Tween-20 (PBST), fixed embryos were permeabilized for 30 min at room temperature in PBS containing 0.5% Triton X-100 and then blocked with 1% bovine serum albumin in PBST for 2 h at room

Figure 1. Intensity of H3K4me1, me2, and me3 in in vivo embryos during preimplantation development. (a) Microscopic images of H3K4me1, me2, and me3 at various developmental stages. Mouse one-cell, two-cell, four-cell, eight-cell, morula, and blastocyst embryos were collected at 18, 42, 50, 62, 76, and 90 h post-hCG injection, respectively, and subjected to immunocytochemistry with the antibody to methylated H3K4. The antibody was localized with FITC-conjugated secondary antibodies (green), and DNA was stained with DAPI (blue). The scale bar denotes 30 μm . (b) Patterns of H3K4me1, me2, and me3 in in vivo embryos. The numbers of embryos examined were 69, 65, 65, 68, 53, and 51 for H3K4me1; 67, 65, 68, 62, 51, and 52 for H3K4me2; and 63, 66, 62, 61, 54, and 56 for H3K4me3 in the one-cell, two-cell, four-cell, eight-cell, morula, and blastocyst embryos, respectively. Quantification of the fluorescence intensity was determined by the ratio of H3K4me to the DNA signal intensity. The data represent mean \pm SEM of three independent experiments. Stages with different superscript letters represent statistically significant differ ($P < 0.05$). BL blastocyst, f female pronucleus, m male pronucleus.



temperature. The embryos then were incubated with primary antibody overnight at 4°C using the following antibodies: polyclonal rabbit anti-H3K4me1 (1/500; 07-436; Upstate Biotechnology, Lake Placid, NY), anti-H3K4me3 (1/600; ab8580; Abcam, Cambridge, MA), anti-KDM5A (1/1,000; 3,876; Cell Signaling Technology, Danvers, MA), anti-KDM5B (1/1,000; 3,273; Cell Signaling Technology), anti-KDM1A (1/600; 2,184; Cell Signaling Technology), anti-ASH2L (1/600; 5,019; Cell Signaling Technology), anti-KMT2B (1/1,000; sc-292359; Santa Cruz Biotechnology, Inc., Santa Cruz, CA), or monoclonal mouse anti-H3K4me2 (1/500; 05-1338; Upstate Biotechnology). After three 30-min washings with PBST, the embryos were incubated with a secondary antibody conjugated with fluorescein isothiocyanate (FITC; 1/300; Jackson ImmunoResearch, West Grove, PA) for 1 h in the dark at room temperature. After washing three times in PBST, the embryos were stained with 4',6-diamidino-2-phenylindole (DAPI; 1 µg/ml; D9542, Sigma) for 15 min, mounted in

Vectashield Mounting Medium (H-1,000; Vector Laboratories, Inc., Burlingame, CA), and sealed with fingernail polish. The slides were examined using a Zeiss Axio Observer microscope equipped with epifluorescence (Carl Zeiss, Oberkochen, Germany). Exposure times from fluorescent light were kept constant for the respective channel (FITC or DAPI). Quantitation of the fluorescence intensity was determined using an image analyzer system, SigmaScan-pro V5.01 (SPSS Inc., Chicago, IL), by the ratios of H3K4me or its regulators to DAPI DNA signals (Shao et al. 2008b).

Statistical analysis. The difference in fluorescence intensity in mouse preimplantation embryos was tested by Kruskal-Wallis nonparametric analysis of variance. The fold change of gene expression between different developmental stages was analyzed by one-way ANOVA using SPSS 11.5 software (SPSS Inc.). Data were presented as mean±SEM of three independent experiments. $P < 0.05$ was considered statistically significant.

Figure 2. Transcription patterns of H3K4 methyltransferases *Setd1a*, *Setd7*, *Kmt2c*, *Ash2l*, *Kmt2b*, *Kmt2a*, and *Ash2l* during mouse preimplantation development. The levels of the transcripts were normalized against *H2afz* and *Gapdh*. The transcript levels of GV oocytes were normalized to 1. The data represent mean±SEM of three independent experiments. Thirty embryos were examined for each gene at various developmental stages. BL blastocyst, 1C one cell, 2C two cell, 4C four cell, 8C eight cell, GV germinal vesicle, MII metaphase II, M morula. For each mRNA within a panel, the values with different superscript letters represent statistically significant differ ($P < 0.05$).

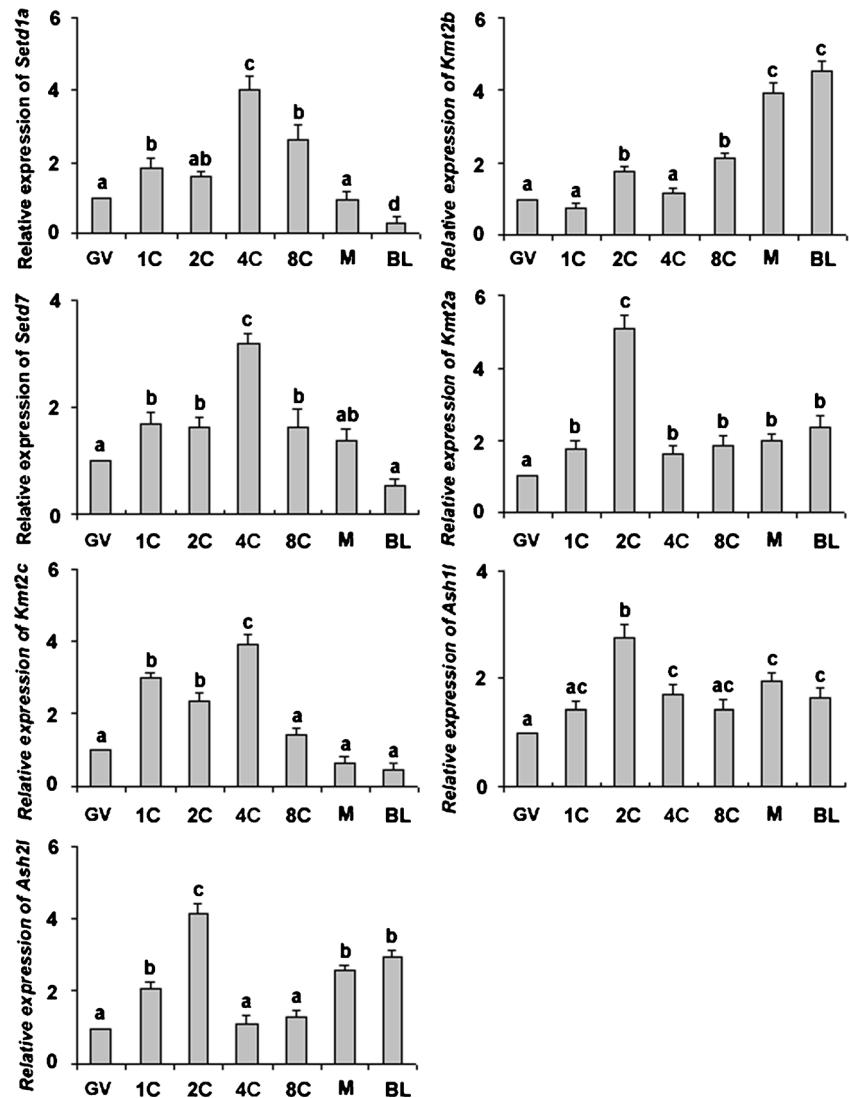
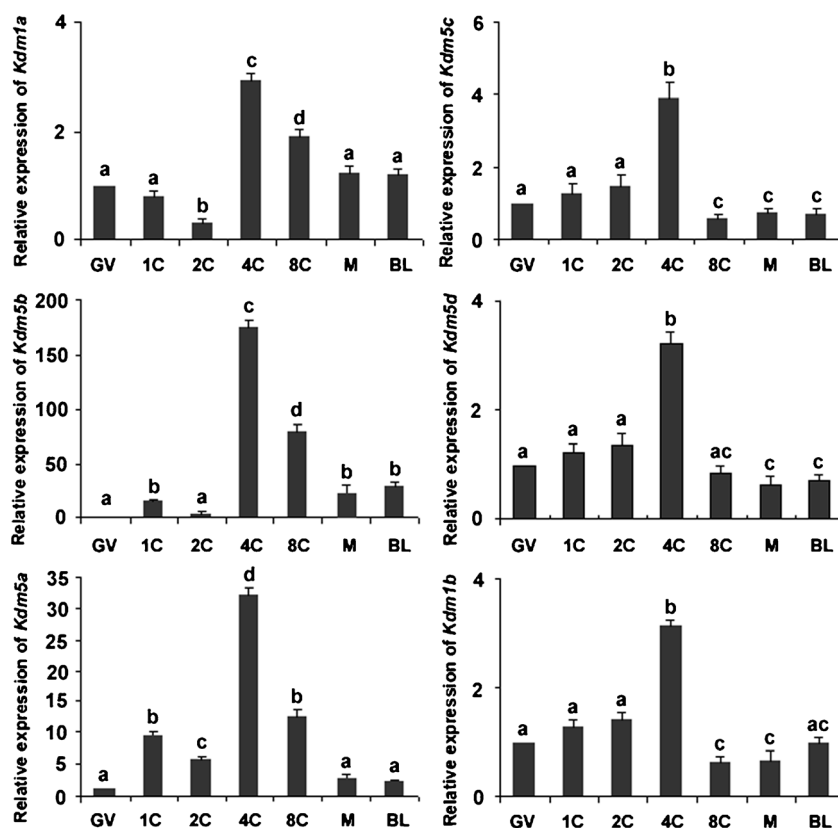


Figure 3. Transcription patterns of H3K4 demethylases *Kdm1a*, *Kdm5b*, *Kdm5a*, *Kdm5c*, *Kdm5d*, and *Kdm1b* during mouse preimplantation development. The levels of the transcripts were normalized against *H2afz* and *Gapdh*. The transcript levels of GV oocytes were normalized to 1. The data represent mean ± SEM of three independent experiments. Thirty embryos were examined for each gene at various developmental stages. For each mRNA within a panel, the values with different superscript letters represent statistically significant differ ($P < 0.05$).



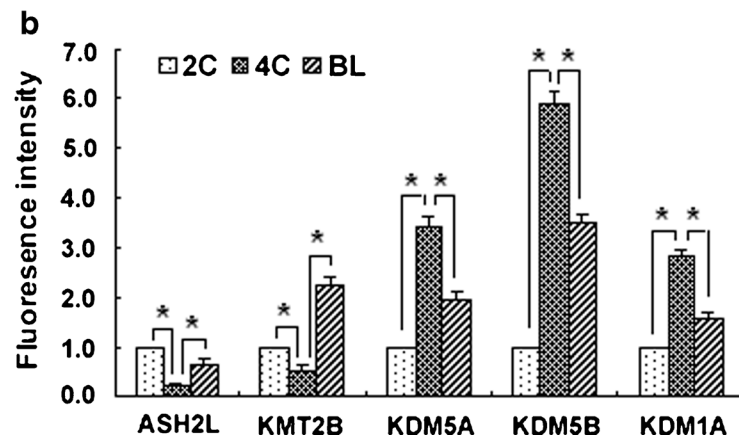
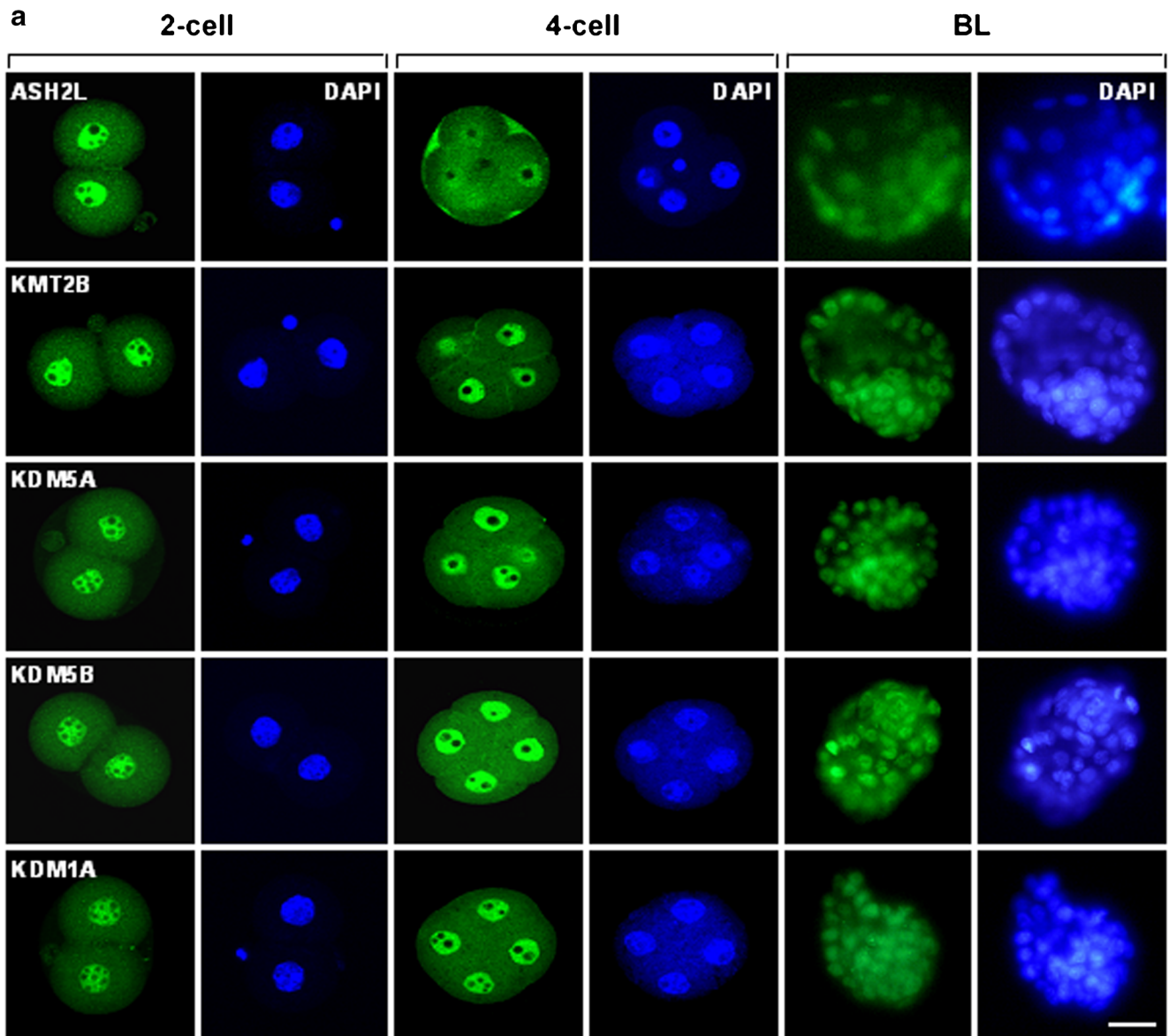
Results

Changes in H3K4me during preimplantation development. To evaluate the profile of H3K4me status during preimplantation development, H3K4me1, me2, and me3 signals were measured at various developmental stages in in vivo mouse embryos. H3K4me1/2/3 signals were observed in female pronuclei, whereas only weak H3K4me2 signal was detected in paternal chromatin (Fig. 1a). Thereafter, intensity of H3K4me2 and me3 signals abruptly increased at the two-cell stage (time of embryonic genome activation, EGA; $P < 0.05$). Subsequently, H3K4me2 signal intensity dramatically decreased at the four-cell stage and remained at low level until the blastocyst stage ($P < 0.05$), whereas H3K4me3 signal intensity transiently decreased at the four-cell stage and then gradually increased to the peak at the blastocyst stage ($P < 0.05$; Fig. 1b). Unlike H3K4me2 and me3, H3K4me1 signal intensity obviously increased at the two-cell stage ($P < 0.05$) but maintained at low level at other developmental stages (Fig. 1b).

mRNA expression of H3K4 methyltransferases and demethylases in preimplantation embryos. Because enzymatic addition of methylated marks is a potential mechanism for the increase in H3K4me levels, we characterized the mRNA expression of H3K4 methyltransferases including *Ash1l*, *Ash2l*, *Kmt2a*, *Kmt2b*, *Kmt2c*, *Setd1a*, and *Setd7*, and of

demethylases including *Kdm1a*, *Kdm1b*, *Kdm5a*, *Kdm5b*, *Kdm5c*, and *Kdm5d* in mouse oocytes and preimplantation embryos using quantitative reverse transcriptase (qRT)-PCR. *Setd1a*, *Setd7*, and *Kmt2c* exhibited a similar expression pattern. Their levels began to increase from the one-cell stage and were highest at the four-cell stage. In the subsequent cell divisions, the levels decreased gradually until the blastocyst stage ($P < 0.05$; Fig. 2). The transcript levels of *Ash2l* were highest in the two-cell embryos, and then showed a significant decrease in the four-cell embryos ($P < 0.05$). From the four- to eight-cell stages, no significant changes in the levels were noted ($P > 0.05$), but significant increases were detected in both morula and blastocyst stages ($P < 0.05$), which is consistent with the pattern of H3K4me2. The *Kmt2b* levels remained relatively low during the stages comprised between the oocytes and the eight-cell embryos, and a stable increase in the levels was observed from the eight-cell embryos until the blastocyst stage ($P < 0.05$; Fig. 2), which is a similar pattern with H3K4me3. Of all the methyltransferase genes, only *Kmt2a* and *Ash1l* displayed a constant level of transcripts at all stages examined except for a relative increase at the two-cell stage ($P < 0.05$).

On the other hand, the expression of *Kdm1a* and *Kdm5b* decreased to the lowest levels at the two-cell stage but increased significantly during subsequent cleavage stages ($P < 0.05$), which is opposite to the level of H3K4me2, whereas the expression of *Kdm5a* remained at low level at the two-



◀ **Figure 4.** Intensity of ASH2L, KMT2B, KDM5A, KDM5B, and KDM1A in in vivo embryos during preimplantation development. (a) Microscopic images of H3K4 methyltransferases ASH2L and KMT2B, and of H3K4 demethylases KDM5A, KDM5B, and KDM1A at the two-cell, four-cell, and blastocyst stages. Mouse two-cell, four-cell, and blastocyst embryos were collected at 42, 50, and 90 h post-hCG injection, respectively. The antibody was localized with FITC-conjugated secondary antibodies (green), and DNA was stained with DAPI (blue). The scale bar denotes 30 μm . (b) Protein expression patterns of ASH2L, KMT2B, KDM5A, KDM5B, and KDM1A in in vivo embryos. The numbers of embryos examined were 62, 57, and 54 for ASH2L; 57, 53, and 51 for KMT2B; 56, 58, and 52 for KDM5A; 59, 54, and 52 for KDM5B; and 61, 56, and 51 for KDM1A in the two-cell, four-cell, and blastocyst embryos, respectively. Quantification of the fluorescence intensity was determined by the ratio of each regulator to the DNA signal intensity. The intensity of fluorescence in the two-cell embryos was normalized to 1. The data represent mean \pm SEM of three independent experiments. The asterisk indicates significant differences between the indicated stages ($P < 0.05$). BL blastocyst.

cell stage, but abruptly increased at the four-cell stage and subsequently decreased to the lowest level at the blastocyst stage ($P < 0.05$; Fig. 3), which is opposite to the H3K4me3 level. Notably, *Kdm5b* was expressed at each stage but very high in the four-cell embryos suggesting a more active transcription state (~ 180 -fold; Fig. 3). In addition, *Kdm5c*, *Kdm5d*, and *Kdm1b* exhibited similar expression patterns—medium level in the one- and two-cell embryos, highest expression in the four-cell embryos, and low expression in the blastocysts (Fig. 3).

Protein expression of H3K4 methyltransferases and demethylases in preimplantation embryos. To specify the correlation between some methyltransferases and demethylases and H3K4me, we measured the signals of ASH2L, KMT2B, KDM5A, KDM5B, and KDM1A at the two-cell, four-cell, and blastocyst stages. The signals were observed at all stages (Fig. 4a), but the quantitative profiles varied between these stages (Fig. 4b). The ASH2L and KMT2B signals had their lowest intensity in the four-cell embryos and the highest intensity in the two-cell embryos for ASH2L and in the blastocysts for KMT2B. The intensity of KDM5A, KDM5B, and KDM1A signals significantly increased to the highest level at the four-cell stage and higher level at the blastocyst stage ($P < 0.05$; Fig. 4b). However, the intensity of KDM5B was markedly higher than that of KDM5A and KDM1A at various stages (Fig. 4b).

Discussion

Histone methylation has emerged as a critical player in the regulation of gene expression (Black et al. 2012). H3K4me is

particularly associated with gene activation (Santos-Rosa et al. 2002), although certain genes can be repressed due to H3K4me promoter occupancy (Wang et al. 2011). This epigenetic state is known to be involved in the regulation of key developmental genes in embryonic stem cells (Wang et al. 2009a, b; Ang et al. 2011) and is involved in the regulation of pluripotency (Pan et al. 2007). Previous studies have confirmed that H3K4me undergoes reprogramming during early embryonic development (Sarmiento et al. 2004; Shao et al. 2008b). However, little information is available on this reprogramming and its regulators in preimplantation embryos. In this study, the profiles of H3K4me and its regulators were investigated during early development of in vivo mouse embryos. At the one-cell stage, H3K4me1/2/3 signals were present in the maternal genome, whereas only weak H3K4me2 signal was observed in the paternal chromatin. Our results are consistent with the previous findings of Sarmiento et al. (2004), van der Heijden et al. (2005), and Black et al. (2012). The difference in H3K4me levels between female and male pronuclei may be responsible for distinctive formation of the respective chromatin. In addition, H3K4me2 and me3 exhibited the highest overall levels at the two-cell and blastocyst stages, respectively, in accordance with the previous reports (Santenard et al. 2010; Wu et al. 2012), indicating that H3K4me2 may play a role in early EGA, whereas H3K4me3 may be involved in initial lineage segregation in the blastocyst.

Histone methylation is catalyzed by a class of enzymes known as histone methyltransferases. We examined the expression of these enzymes during preimplantation development to elucidate which enzymes are involved in regulating H3K4me during this period. A previous study reported that *Ash2l* presented relatively high transcript levels during the EGA in in vitro porcine embryos from a microarray analysis (Whitworth et al. 2005). This result was confirmed in the present study by using a different animal species and the qRT-PCR and immunocytochemical staining. The high levels of *Ash2l* around the EGA were consistent with that of H3K4me2, which may stabilize this methylation levels during the EGA. A relative decrease in expression of *Kmt2a* was detected in another study (Gao et al. 2010). The peak in expression we observe at the two-cell stage is thus intriguing and should be investigated in further studies. Recently, Andreu-Vieyra et al. (2010) reported that *Kmt2b* transcripts exhibited higher level at the morula and blastocyst stages in in vitro mouse embryos. This result is consistent with our finding that the highest levels of *Kmt2b* mRNA were observed in in vivo mouse embryos at the same stages, suggesting that it may play a role in the initial cell lineage separation by means of methylating H3K4.

Removal of H3K4me by specific demethylases is crucial for gene repression to occur. Hence, it was expected that this histone methylation would be activated in order to allow for the EGA. This was to some degree substantiated, as the levels

of H3K4me2 increased from the one- to two-cell stages. Correspondingly, a concomitant decrease in the mRNA and protein levels of its demethylases, *Kdm5b* and *Kdm1a*, was observed. This was in accordance with the recent results obtained by McGraw et al. (2007). Interestingly, the protein levels of KDM5B were the highest in the four-cell embryos, but its levels were only six times higher than that in the two-cell embryos. The mRNA levels of *Kdm5b* were at least 40 times higher in the four-cell embryos. It is possible that KDM5B causes a feedback inhibition of the splicing of the transcript of its own gene in the four-cell embryos. Another possibility is that post-translation modifications of KDM5B protein during the translation block the translation process or promote the degradation of the protein itself. In addition, McGraw et al. (2007) also found that a decrease in expression of *Kdm5a* was detected in the morula and blastocysts which reflects a similar pattern observed in our expression data which shows this reduced expression persists at the blastocyst stage. Noteworthy, the protein levels of KDM5A at the blastocyst stage was about two times higher than that at the two-cell stage, while the mRNA levels of *Kdm5a* were lower at the blastocyst stage. A possible explanation for this phenotype is that an increased availability of active KDM5A by unknown kinases may promote the translation of itself mRNA by virtue of upstream open reading frames (ORFS) in their 5' untranslated regions (UTRs). Another possibility is that KDM5A itself causes a feedback inhibition of the transcription of its own gene.

Based on these findings, we suggest that H3K4me2 may play a role in the EGA. Hence, relatively high levels of this permissive histone modification coinciding with a peak expression of its methyltransferase, ASH2L, were noted at the two-cell stage, whereas a decrease in expression of its demethylases, KDM5B and KDM1A, was observed. H3K4me3 may play a major role in lineage segregation in the blastocyst when it occurs at relatively high levels that associate with the expression of KMT2B and KDM5A. For future studies, it will be interesting to investigate whether the depletions of these enzymes by RNAi change the H3K4me levels and therefore affect embryonic development.

Acknowledgments This work was supported by grants from the National Natural Science Foundation of China (81170573) and the Open Research Fund Program of Jiangsu Provincial Key Laboratory for Science and Technology of Photon Manufacturing (Jiangsu University) (GZ200710) and the Natural Science Foundation of Jiangsu Province (BK2011485).

References

- Albert M, Schmitz SU, Kooistra SM, Malatesta M, Morales Torres C, Rekling JC, Johansen JV, Abarrategui I, Helin K (2013) The histone demethylase Jarid1b ensures faithful mouse development by protecting developmental genes from aberrant H3K4me3. *PLoS Genet* 9:e1003461
- Andreu-Vieyra CV, Chen R, Agno JE, Glaser S, Anastassiadis K, Stewart AF, Matzuk MM (2010) MLL2 is required in oocytes for bulk histone 3 lysine 4 trimethylation and transcriptional silencing. *PLoS Biol* 8:e1000453
- Ang YS, Tsai SY, Lee DF, Monk J, Su J, Ratnakumar K, Ding J, Ge Y, Darr H, Chang B, Wang J, Rendl M, Bernstein E, Schaniel C, Lemischka IR (2011) Wdr5 mediates self-renewal and reprogramming via the embryonic stem cell core transcriptional network. *Cell* 145:183–197
- Barski A, Cuddapah S, Cui K, Roh TY, Schones DE, Wang Z, Wei G, Chepelev I, Zhao K (2007) High-resolution profiling of histone methylations in the human genome. *Cell* 129:823–837
- Beisel C, Paro R (2011) Silencing chromatin: comparing modes and mechanisms. *Nat Rev Genet* 12:123–135
- Bernstein BE, Mikkelsen TS, Xie X, Kamal M, Huebert DJ, Cuff J, Fry B, Meissner A, Wernig M, Plath K, Jaenisch R, Wagschal A, Feil R, Schreiber SL, Lander ES (2006) A bivalent chromatin structure marks key developmental genes in embryonic stem cells. *Cell* 125:315–326
- Black JC, Van Rechem C, Whetstone JR (2012) Histone lysine methylation dynamics: establishment, regulation, and biological impact. *Mol Cell* 48:491–507
- Chan SW, Hong W (2001) Retinoblastoma-binding protein 2 (Rbp2) potentiates nuclear hormone receptor-mediated transcription. *J Biol Chem* 276:28402–28412
- Ciccone DN, Su H, Hevi S, Gay F, Lei H, Bajko J, Xu G, Li E, Chen T (2009) KDM1B is a histone H3K4 demethylase required to establish maternal genomic imprints. *Nature* 461:415–418
- Di Stefano L, Ji JY, Moon NS, Herr A, Dyson N (2007) Mutation of *Drosophila* Lsd1 disrupts H3-K4 methylation, resulting in tissue-specific defects during development. *Curr Biol* 17:808–812
- Dillon SC, Zhang X, Trievel RC, Cheng X (2005) The SET-domain protein superfamily: protein lysine methyltransferases. *Genome Biol* 6:227
- Dou Y, Milne TA, Ruthenburg AJ, Lee S, Lee JW, Verdine GL, Allis CD, Roeder RG (2006) Regulation of MLL1 H3K4 methyltransferase activity by its core components. *Nat Struct Mol Biol* 13:713–719
- Eissenberg JC, Shilatifard A (2010) Histone H3 lysine 4 (H3K4) methylation in development and differentiation. *Dev Biol* 339:240–249
- Eliazer S, Shalaby NA, Buszczak M (2011) Loss of lysine-specific demethylase 1 nonautonomously causes stem cell tumors in the *Drosophila* ovary. *Proc Natl Acad Sci U S A* 108:7064–7069
- Fang R, Barbera AJ, Xu Y, Rutenberg M, Leonor T, Bi Q, Lan F, Mei P, Yuan GC, Lian C, Peng J, Cheng D, Sui G, Kaiser UB, Shi Y, Shi YG (2010) Human LSD2/KDM1b/AOF1 regulates gene transcription by modulating intragenic H3K4me2 methylation. *Mol Cell* 39:222–233
- Gao Y, Hyttel P, Hall VJ (2010) Regulation of H3K27me3 and H3K4me3 during early porcine embryonic development. *Mol Reprod Dev* 77: 540–549
- Greer EL, Maures TJ, Hauswirth AG, Green EM, Leeman DS, Maro GS, Han S, Banko MR, Gozani O, Brunet A (2010) Members of the H3K4 trimethylation complex regulate lifespan in a germline-dependent manner in *C. elegans*. *Nature* 466:383–387
- Gregory GD, Vakoc CR, Rozovskaia T, Zheng X, Patel S, Nakamura T, Canaani E, Blobel GA (2007) Mammalian ASH1L is a histone methyltransferase that occupies the transcribed region of active genes. *Mol Cell Biol* 27:8466–8479
- Heintzman ND, Stuart RK, Hon G, Fu Y, Ching CW, Hawkins RD, Barrera LO, Van Calcar S, Qu C, Ching KA, Wang W, Weng Z, Green RD, Crawford GE, Ren B (2007) Distinct and predictive chromatin signatures of transcriptional promoters and enhancers in the human genome. *Nat Genet* 39:311–318
- Jensen LR, Amende M, Gurok U, Moser B, Gimmel V, Tzschach A, Janecke AR, Tariverdian G, Chelly J, Fryns JP, Van Esch H, Kleefstra T, Hamel B, Moraine C, Geck J, Turner G, Reinhardt R,

- Kalscheuer VM, Ropers HH, Lenzner S (2005) Mutations in the JARID1C gene, which is involved in transcriptional regulation and chromatin remodeling, cause X-linked mental retardation. *Am J Hum Genet* 76:227–236
- Katz DJ, Edwards TM, Reinke V, Kelly WG (2009) A *C. elegans* LSD1 demethylase contributes to germline immortality by reprogramming epigenetic memory. *Cell* 137:308–320
- Klose RJ, Kallin EM, Zhang Y (2006) JmjC-domain-containing proteins and histone demethylation. *Nat Rev Genet* 7:715–727
- Lee J, Saha PK, Yang QH, Lee S, Park JY, Suh Y, Lee SK, Chan L, Roeder RG, Lee JW (2008) Targeted inactivation of MLL3 histone H3-Lys-4 methyltransferase activity in the mouse reveals vital roles for MLL3 in adipogenesis. *Proc Natl Acad Sci U S A* 105:19229–19234
- Lee JH, Skalnik DG (2008) Wdr82 is a C-terminal domain-binding protein that recruits the Setd1A histone H3-Lys4 methyltransferase complex to transcription start sites of transcribed human genes. *Mol Cell Biol* 28:609–618
- Mamo S, Gal AB, Bodo S, Dinnyes A (2007) Quantitative evaluation and selection of reference genes in mouse oocytes and embryos cultured in vivo and in vitro. *BMC Dev Biol* 7:14
- McGraw S, Vigneault C, Sirard MA (2007) Temporal expression of factors involved in chromatin remodeling and in gene regulation during early bovine in vitro embryo development. *Reproduction* 133:597–608
- Mikkelsen TS, Ku M, Jaffe DB, Issac B, Lieberman E, Giannoukos G, Alvarez P, Brockman W, Kim TK, Koche RP, Lee W, Mendenhall E, O'Donovan A, Presser A, Russ C, Xie X, Meissner A, Wernig M, Jaenisch R, Nusbaum C, Lander ES, Bernstein BE (2007) Genome-wide maps of chromatin state in pluripotent and lineage-committed cells. *Nature* 448:553–560
- Milne TA, Briggs SD, Brock HW, Martin ME, Gibbs D, Allis CD, Hess JL (2002) MLL targets SET domain methyltransferase activity to *Hox* gene promoters. *Mol Cell* 10:1107–1117
- Pan G, Tian S, Nie J, Yang C, Ruotti V, Wei H, Jonsdottir GA, Stewart R, Thomson JA (2007) Whole-genome analysis of histone H3 lysine 4 and lysine 27 methylation in human embryonic stem cells. *Cell Stem Cell* 1:299–312
- Pradhan S, Chin HG, Esteve PO, Jacobsen SE (2009) SET7/9 mediated methylation of non-histone proteins in mammalian cells. *Epigenetics* 4:383–387
- Santenard A, Ziegler-Birling C, Koch M, Tora L, Bannister AJ, Torres-Padilla ME (2010) Heterochromatin formation in the mouse embryo requires critical residues of the histone variant H3.3. *Nat Cell Biol* 12:853–862
- Santos-Rosa H, Schneider R, Bannister AJ, Sherriff J, Bernstein BE, Emre NC, Schreiber SL, Mellor J, Kouzarides T (2002) Active genes are tri-methylated at K4 of histone H3. *Nature* 419:407–411
- Sarmiento OF, Digilio LC, Wang Y, Perlin J, Herr JC, Allis CD, Coonrod SA (2004) Dynamic alterations of specific histone modifications during early murine development. *J Cell Sci* 117:4449–4459
- Shao GB, Ding HM, Gong AH (2008a) Role of histone methylation in zygotic genome activation in the preimplantation mouse embryo. *In Vitro Cell Dev Biol Anim* 44:115–120
- Shao GB, Ding HM, Gong AH, Xiao DS (2008b) Inheritance of histone H3 methylation in reprogramming of somatic nuclei following nuclear transfer. *J Reprod Dev* 54:233–238
- Shi Y, Lan F, Matson C, Mulligan P, Whetstone JR, Cole PA, Casero RA, Shi Y (2004) Histone demethylation mediated by the nuclear amine oxidase homolog LSD1. *Cell* 119:941–953
- Smith JA, White EA, Sowa ME, Powell ML, Ottinger M, Harper JW, Howley PM (2010) Genome-wide siRNA screen identifies SMCX, EP400, and Brd4 as E2-dependent regulators of human papillomavirus oncogene expression. *Proc Natl Acad Sci U S A* 107:3752–3757
- Stoller JZ, Huang L, Tan CC, Huang F, Zhou DD, Yang J, Gelb BD, Epstein JA (2010) Ash2l interacts with Tbx1 and is required during early embryogenesis. *Exp Biol Med (Maywood)* 235:569–576
- Terranova R, Agherbi H, Boned A, Meresse S, Djabali M (2006) Histone and DNA methylation defects at *Hox* genes in mice expressing a SET domain-truncated form of Mll. *Proc Natl Acad Sci U S A* 103:6629–6634
- van der Heijden GW, Dieker JW, Derijck AA, Muller S, Berden JH, Braat DD, van der Vlag J, de Boer P (2005) Asymmetry in histone H3 variants and lysine methylation between paternal and maternal chromatin of the early mouse zygote. *Mech Dev* 122:1008–1022
- VerMilyea MD, O'Neill LP, Turner BM (2009) Transcription-independent heritability of induced histone modifications in the mouse preimplantation embryo. *PLoS One* 4:e6086
- Wan M, Liang J, Xiong Y, Shi F, Zhang Y, Lu W, He Q, Yang D, Chen R, Liu D, Barton M, Songyang Z (2013) The trithorax group protein Ash2l is essential for pluripotency and maintaining open chromatin in embryonic stem cells. *J Biol Chem* 288:5039–5048
- Wang J, Hevi S, Kurash JK, Lei H, Gay F, Bajko J, Su H, Sun W, Chang H, Xu G, Gaudet F, Li E, Chen T (2009a) The lysine demethylase LSD1 (KDM1) is required for maintenance of global DNA methylation. *Nat Genet* 41:125–129
- Wang J, Zhang M, Zhang Y, Kou Z, Han Z, Chen DY, Sun QY, Gao S (2010) The histone demethylase JMJD2C is stage-specifically expressed in preimplantation mouse embryos and is required for embryonic development. *Biol Reprod* 82:105–111
- Wang K, Chen Y, Chang EA, Knott JG, Cibelli JB (2009b) Dynamic epigenetic regulation of the Oct4 and Nanog regulatory regions during neural differentiation in rhesus nuclear transfer embryonic stem cells. *Cloning Stem Cells* 11:483–496
- Wang SS, Zhou BO, Zhou JQ (2011) Histone H3 lysine 4 hypermethylation prevents aberrant nucleosome remodeling at the PHO5 promoter. *Mol Cell Biol* 31:3171–3181
- Whitworth KM, Agca C, Kim JG, Patel RV, Springer GK, Bivens NJ, Forrester LJ, Mathialagan N, Green JA, Prather RS (2005) Transcriptional profiling of pig embryogenesis by using a 15-K member unigene set specific for pig reproductive tissues and embryos. *Biol Reprod* 72:1437–1451
- Wu FR, Liu Y, Shang MB, Yang XX, Ding B, Gao JG, Wang R, Li WY (2012) Differences in H3K4 trimethylation in in vivo and in vitro fertilization mouse preimplantation embryos. *Genet Mol Res* 11:1099–1108
- Xiang Y, Zhu Z, Han G, Ye X, Xu B, Peng Z, Ma Y, Yu Y, Lin H, Chen AP, Chen CD (2007) JARID1B is a histone H3 lysine 4 demethylase up-regulated in prostate cancer. *Proc Natl Acad Sci U S A* 104:19226–19231
- Yamane K, Tateishi K, Klose RJ, Fang J, Fabrizio LA, Erdjument-Bromage H, Taylor-Papadimitriou J, Tempst P, Zhang Y (2007) PLU-1 is an H3K4 demethylase involved in transcriptional repression and breast cancer cell proliferation. *Mol Cell* 25:801–812